Journal of Power Sources 233 (2013) 231–235

Contents lists available at SciVerse ScienceDirect

Journal of Power Sources

journal homepage: www.elsevier.com/locate/jpowsour

Short communication

All-solid-state lithium secondary batteries using the $75Li_2S{\cdot}25P_2S_5$ glass and the $70Li_2S{\cdot}30P_2S_5$ glass–ceramic as solid electrolytes

Takamasa Ohtomo [a,b,*], Akitoshi Hayashi [a], Masahiro Tatsumisago [a], Yasushi Tsuchida [b], Shigenori Hama [b], Koji Kawamoto [b]

[a] Department of Applied Chemistry, Graduate School of Engineering, Osaka Prefecture University, 1-1 Gakuen-cho, Naka-ku, Sakai, Osaka 599-8531, Japan
[b] Battery Research Division, Toyota Motor Corporation, Higashifuji Technical Center, 1200 Mishuku, Susono, Shizuoka 410-1193, Japan

HIGHLIGHTS

- Characteristics of solid electrolytes affect cell performance.
- Conductivities of electrolytes have an effect on rate performance of cells.
- Increasing chemical stabilities of electrolytes improves cycle performance of cells.
- Both high conductivities and high chemical stabilities are desired for electrolytes.

ARTICLE INFO

Article history:
Received 27 August 2012
Received in revised form
28 November 2012
Accepted 16 January 2013
Available online 26 January 2013

Keywords:
All-solid-state battery
Sulfide solid electrolyte
Chemical stability
Lithium ion conductivity
Interface

ABSTRACT

The $70Li_2S{\cdot}30P_2S_5$ glass–ceramic showed high ion conductivity of 1.5×10^{-3} S cm^{-1} at room temperature. The $75Li_2S{\cdot}25P_2S_5$ glass showed ion conductivity of 5.0×10^{-4} S cm^{-1} at room temperature and high chemical stability. All-solid-state C/$LiCoO_2$ cells using those materials as solid electrolytes were assembled. Their cell performance were compared. The cell using the $70Li_2S{\cdot}30P_2S_5$ glass–ceramic showed superior rate performance to the cell using the $75Li_2S{\cdot}25P_2S_5$ glass. On the other hand, the cell using the $75Li_2S{\cdot}25P_2S_5$ glass showed superior cycle performance to the cell using the $70Li_2S{\cdot}30P_2S_5$ glass–ceramic. It was suggested that solid electrolytes in all-solid-state batteries preferably had both high ion conductivity and high chemical stability.

1. Introduction

All-solid-state lithium secondary batteries are one candidate of high-energy-density batteries because of their high flexibility of battery forms. Realization of all-solid-state batteries demands high lithium ion conductors. Sulfide solid electrolytes showed high lithium ion conductivities of 10^{-4} to 10^{-2} S cm^{-1} at room temperature [1–6]. An earlier report described that the $70Li_2S{\cdot}30P_2S_5$ (mol%) glass–ceramic showed the highest lithium ion conductivity of 3.2×10^{-3} S cm^{-1} at room temperature in the system Li_2S–P_2S_5 [4]. However, most sulfide solid electrolytes with high ion conductivities have low chemical stability to moisture in air because sulfide materials tend to hydrolyze and generate H_2S gas in air. The $75Li_2S{\cdot}25P_2S_5$ glass showed the highest chemical stability in the system Li_2S–P_2S_5 because the H_2S gas generation from this glass in air was the least in the system Li_2S–P_2S_5 [7]. It was confirmed that all-solid-state cells using these Li_2S–P_2S_5 solid electrolytes operated well as lithium secondary batteries at room temperature [8,9]. However, effects of solid electrolyte characteristics on cell performance remain unclear.

In this study, electrochemical performance of all-solid-state cells using two kinds of Li_2S–P_2S_5 solid electrolytes with different characteristics was investigated. The $70Li_2S{\cdot}30P_2S_5$ glass–ceramic with the high conductivity and the $75Li_2S{\cdot}25P_2S_5$ glass with the high chemical stability were used for the cells. Rate and cycle performance in both cells was compared. Furthermore, solid–solid interfaces between $LiCoO_2$ positive electrodes and the sulfide solid electrolytes were analyzed to study the relation between cell performance and solid electrolyte characteristics.

* Corresponding author. Battery Research Division, Toyota Motor Corporation, Higashifuji Technical Center, 1200 Mishuku, Susono, Shizuoka 410-1193, Japan. Tel.: +81 55 997 9661; fax: +81 55 997 7879.
E-mail addresses: takamasa@ohtomo.tec.toyota.co.jp, takamasa44@yahoo.co.jp (T. Ohtomo).

0378-7753/$ – see front matter © 2013 Elsevier B.V. All rights reserved.
http://dx.doi.org/10.1016/j.jpowsour.2013.01.090

2. Experimental

The $70Li_2S{\cdot}30P_2S_5$ glass–ceramic was prepared by mechanical milling using a planetary ball mill apparatus and consecutive heat treatment [4]. The $75Li_2S{\cdot}25P_2S_5$ glass was prepared by mechanical milling [3]. For the preparation of Li_2S–P_2S_5 solid electrolytes, crystalline powders of Li_2S (Nippon Chemical Industrial Co. Ltd., 99.9%) and P_2S_5 (Aldrich Chemical Co. Inc., 99%) were used as starting materials. A mixture of the starting materials was loaded into a zirconia pot in 45 mL volume with 10 zirconia balls of 10 mm diameter. The pot was mounted in the planetary ball mill apparatus (Pulverisette 7, Fritsch) and milled at 370 rpm for 40 h to obtain glassy materials. The heat treatment of the $70Li_2S{\cdot}30P_2S_5$ powder glass at 290 °C was conducted to prepare the glass–ceramic. Conductivities of sulfide solid electrolytes were determined using pellets obtained by cold pressing under 4 ton cm^{-2}. The $70Li_2S{\cdot}30P_2S_5$ glass–ceramic and the $75Li_2S{\cdot}25P_2S_5$ glass showed conductivities of 1.5×10^{-3} and 5.0×10^{-4} S cm^{-1} at room temperature, respectively. The conductivity of the $70Li_2S{\cdot}30P_2S_5$ glass–ceramic was lower than that in our previous report [4]. The conductivity of the heat-treated pellet was measured in our previous report. Glass generally softens above the glass transition temperature, which is lower than the crystallization temperature. Consequently, the heat-treated pellet in our previous report was denser than the pellet obtained by cold pressing in this study. Therefore, the $70Li_2S{\cdot}30P_2S_5$ glass–ceramic in this study showed the lower conductivity, compared to our previous study. On the other hand, the conductivity of the $75Li_2S{\cdot}25P_2S_5$ glass in this study was higher than that in our previous report [3]. This would be caused by the difference of materials of pots and balls used for the synthesis. Zirconia pots and balls were used for mechanical milling in this study. Alumina pots and balls were used for mechanical milling in our previous study [3].

Ota et al. reported that large interfacial resistance between $LiCoO_2$ positive electrodes and sulfide solid electrolytes was greatly decreased by $LiCoO_2$ coated with $LiNbO_3$ or $Li_4Ti_5O_{12}$ [10]. Similarly, in this study, $LiCoO_2$ particles were coated with $LiNbO_3$ by spray coating as described below. The $LiNbO_3$ coating layer was formed from ethanol solution of alkoxides of Li and Nb. The coating solution was prepared by mixing $LiOC_2H_5$ (12.6 g), $Nb(OC_2H_5)_5$ (77.6 g) and anhydrous ethanol (609.8 g). $LiOC_2H_5$ (Kojundo Chemical Lab. Co. Ltd., 99.9%), $Nb(OC_2H_5)_5$ (Kojundo Chemical Lab. Co. Ltd., 99.99%), and anhydrous ethanol (Wako Pure Chemical Industries Ltd., 99.5%) were used as starting materials. The solution was sprayed onto the surface of the $LiCoO_2$ particles (Toda Kogyo Corp.) using a rolling fluidized coating machine (SFD-01, Powrex). After the coating, the samples were heated at 400 °C for 30 min in air. Laboratory-scale solid-state cells were fabricated in the following manner. Mixtures of the $LiCoO_2$ particles coated with $LiNbO_3$ and the sulfide solid electrolyte powders with a weight ratio of 70:30 were used as composite positive electrode materials. Mixtures of natural graphite (Mitsubishi Chemical Corp.) powders and the sulfide solid electrolyte powders with a weight ratio of 50:50 were used as composite negative electrode materials. A triple-layer pellet, consisting of composite positive electrode materials (16.2 mg), solid electrolytes (65.0 mg), and composite negative electrode materials (12.0 mg), was obtained by pressing under 4 ton cm^{-2}. That pellet was sandwiched and held by two stainless-steel rods as current collectors. The loading of $LiCoO_2$ (theoretical capacity; 137 mA h g^{-1}) was 11.3 mg, and the capacity of the positive electrode composite was 1.55 mA h. The loading of graphite (theoretical capacity; 372 mA h g^{-1}) was 6 mg, and the capacity of the negative electrode composite was 2.23 mA h. Consequently, charge–discharge measurements of the cells were controlled by the capacity of the positive electrode composite. The current density of 1 C rate was 1.55 mA. The capacity of the cell in this study means the capacity normalized by the weight of $LiCoO_2$.

The cells were charged and discharged using a charge–discharge measuring device (TOSCAT3200, Toyo System Co., Ltd.). Rate performance of the cells was evaluated under several current density from 0.1 C to 10 C at room temperature. Cycle performance of the cells was evaluated under current density of 0.1 C at 60 °C. Changes of the cell resistances in charge–discharge cycles were also measured using an impedance analyzer (SI1260; Solartron Analytical). Furthermore, interfaces between the $LiCoO_2$ positive electrodes and the sulfide solid electrolytes were observed using transmission electron microscopy (TEM) and scanning TEM (STEM) with energy dispersive X-ray spectroscopy (EDX) after the cells were kept at a voltage of 4.0 V at 60 °C for 4 weeks. Samples for TEM observation were prepared using focused ion beam (FIB). All processes without $LiNbO_3$ coating onto the $LiCoO_2$ particles were performed in a dry Ar atmosphere ($[H_2O] < 1$ ppm).

3. Results and discussion

Fig. 1 shows charge–discharge curves of the all-solid-state C/$LiCoO_2$ cells using the $70Li_2S{\cdot}30P_2S_5$ glass–ceramic and the $75Li_2S{\cdot}25P_2S_5$ glass as solid electrolytes. The cells were charged to 4.1 V and discharged to 3.0 V. Both cells operate as secondary batteries. Discharge capacity of 90 and 100 mA h g^{-1} is obtained for the cells using the $70Li_2S{\cdot}30P_2S_5$ glass–ceramic and the $75Li_2S{\cdot}25P_2S_5$ glass, respectively.

Fig. 2 shows rate performance of the all-solid-state C/$LiCoO_2$ cells using the $70Li_2S{\cdot}30P_2S_5$ glass–ceramic and the $75Li_2S{\cdot}25P_2S_5$ glass at room temperature. The cell using the $70Li_2S{\cdot}30P_2S_5$ glass–ceramic is discharged even at high current density of 10 C, although the cell using the $75Li_2S{\cdot}25P_2S_5$ glass is discharged at current density of 5 C. It is estimated that the cell using the $70Li_2S{\cdot}30P_2S_5$ glass–ceramic showed superior rate performance because ion conductivity of the $70Li_2S{\cdot}30P_2S_5$ glass–ceramic was higher than that of the $75Li_2S{\cdot}25P_2S_5$ glass at room temperature.

Fig. 3 shows impedance plots of the all-solid-state C/$LiCoO_2$ cells using the $70Li_2S{\cdot}30P_2S_5$ glass–ceramic and the $75Li_2S{\cdot}25P_2S_5$ glass after charging at voltage of 4.0 V at room temperature. Cell voltages were adjusted by constant voltage charging for 20 h. A lower intersection of semicircles and the

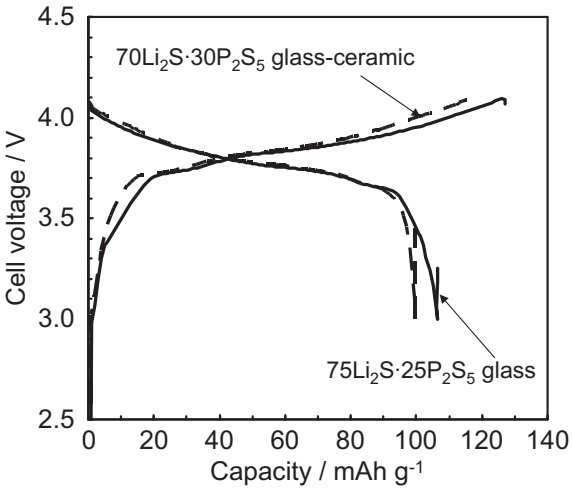

Fig. 1. Charge–discharge curves of the all-solid-state C/$LiCoO_2$ cells using the $70Li_2S{\cdot}30P_2S_5$ glass–ceramic and the $75Li_2S{\cdot}25P_2S_5$ glass at room temperature. Measurements were conducted at 0.1 C in the voltage range of 3.0–4.1 V.

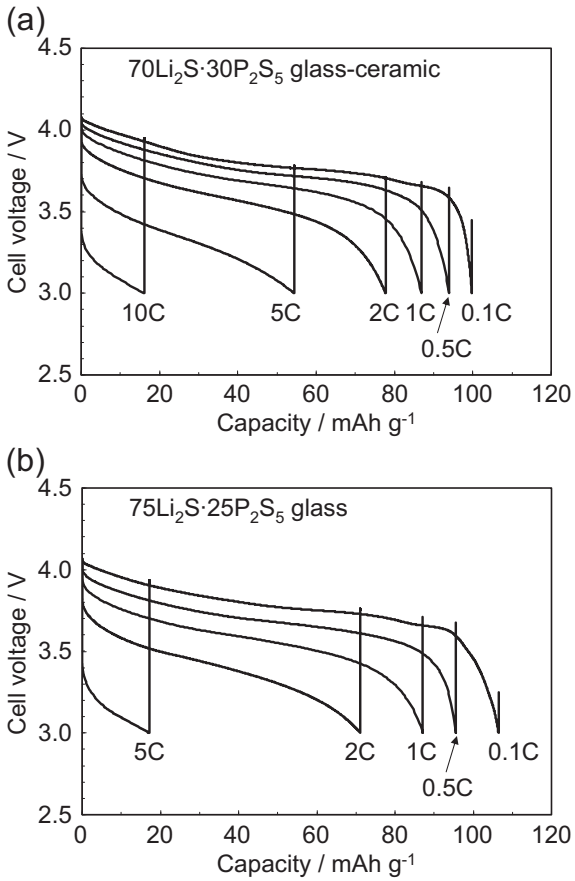

Fig. 2. Discharge curves of the all-solid-state C/$LiCoO_2$ cells using the $70Li_2S{\cdot}30P_2S_5$ glass–ceramic (a) and the $75Li_2S{\cdot}25P_2S_5$ glass (b) at room temperature. The cells were charged to 4.1 V at 0.1 C and were discharged to 3.0 V at 0.1–10 C.

real axis in the impedance plots corresponded to resistance of a solid electrolyte layer: R_a in Fig. 3. A diameter of semicircles in the impedance plots was attributed to interfacial resistance between $LiCoO_2$ and sulfide solid electrolytes: R_b in Fig. 3 [11]. The resistance attributable to the solid electrolyte layer, R_a, in the cell using the $75Li_2S{\cdot}25P_2S_5$ glass is about three times higher than that in the cell using the $70Li_2S{\cdot}30P_2S_5$ glass–ceramic because ion conductivity of the $70Li_2S{\cdot}30P_2S_5$ glass–ceramic was about three times higher than that of the $70Li_2S{\cdot}30P_2S_5$ glass–ceramic in this study. On the other hand, the interfacial resistance, R_b, between $LiCoO_2$ and sulfide solid electrolytes of the cell using the $70Li_2S{\cdot}30P_2S_5$ glass–ceramic is larger than that of the cell using the $75Li_2S{\cdot}25P_2S_5$ glass. It is suggested that the interfacial resistance is not governed by only ion conductivity of solid electrolytes.

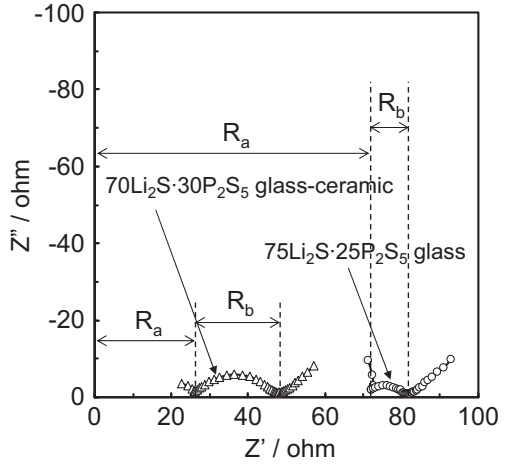

Fig. 3. Impedance plots of the all-solid-state C/$LiCoO_2$ cells using the $70Li_2S{\cdot}30P_2S_5$ glass–ceramic and the $75Li_2S{\cdot}25P_2S_5$ glass at voltage of 4.0 V.

Fig. 4 shows cycle performance of the all-solid-state C/$LiCoO_2$ cells using the $70Li_2S{\cdot}30P_2S_5$ glass–ceramic and the $75Li_2S{\cdot}25P_2S_5$ glass at 60 °C under current density of 0.1 C. Triangles and circles denote the cell using the $70Li_2S{\cdot}30P_2S_5$ glass–ceramic and the cell using the $75Li_2S{\cdot}25P_2S_5$ glass, respectively. Discharge capacity of both cells decreases during charge–discharge cycles, although the excellent cycle performance of the In/$80Li_2S{\cdot}20P_2S_5$ glass–ceramic/$LiCoO_2$ cell at room temperature was reported in our previous study [12]. Capacity fading observed in this study might be caused by graphite as negative electrode materials and operating at the high temperature of 60 °C. The cycle performance of the cell using the $75Li_2S{\cdot}25P_2S_5$ glass is superior to that of the cell using the $70Li_2S{\cdot}30P_2S_5$ glass–ceramic. The discharge capacity after 100 cycles of the cell using the $75Li_2S{\cdot}25P_2S_5$ glass is 65% of the initial capacity, whereas that of the cell using the $70Li_2S{\cdot}30P_2S_5$ glass–ceramic is 42%. On the other hand, a capacity drop is slightly observed at every 10 cycles for the cell with the $70Li_2S{\cdot}30P_2S_5$ glass-ceramic. The capacity drop would result from rest time for the impedance measurements at every 10 cycles. Impedance results are showed in Fig. 5. The impedance measurements of all cells were performed at the same time. Charge–discharge cycles of the smaller capacity cells were completed more quickly, and were kept at 60 °C for a longer time. The capacity of the cell using the $70Li_2S{\cdot}30P_2S_5$ glass–ceramic is less than that of the cell using the $75Li_2S{\cdot}25P_2S_5$ glass in all cycles. The rest time of the cell using the $70Li_2S{\cdot}30P_2S_5$ glass–ceramic was therefore longer than that of the cell using the $75Li_2S{\cdot}25P_2S_5$ glass. Thus, the interfacial resistance of the cell using the $70Li_2S{\cdot}30P_2S_5$ glass–ceramic increased rapidly while the temperature was maintained at 60 °C; details are discussed later.

Fig. 5 shows changes of interfacial resistance between $LiCoO_2$ and sulfide solid electrolytes during charge–discharge cycles at

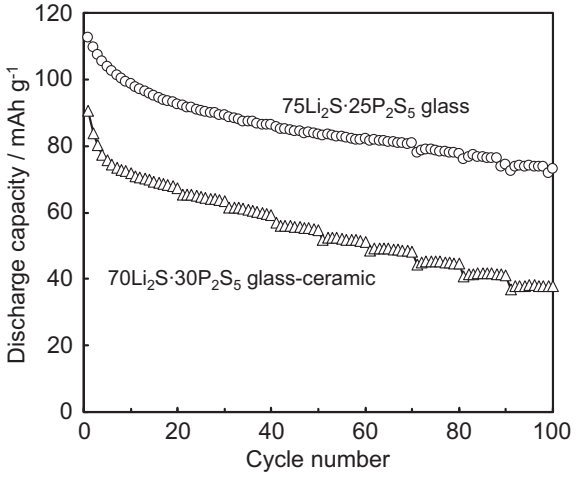

Fig. 4. Cycle performance of the all-solid-state C/$LiCoO_2$ cells using the $70Li_2S{\cdot}30P_2S_5$ glass–ceramic and the $75Li_2S{\cdot}25P_2S_5$ glass at 60 °C. Charge–discharge cycles were carried out at 0.1 C in the voltage range of 3.0–4.1 V. Triangles and circles denote data for the cell using the $70Li_2S{\cdot}30P_2S_5$ glass–ceramic and the cell using the $75Li_2S{\cdot}25P_2S_5$ glass, respectively.

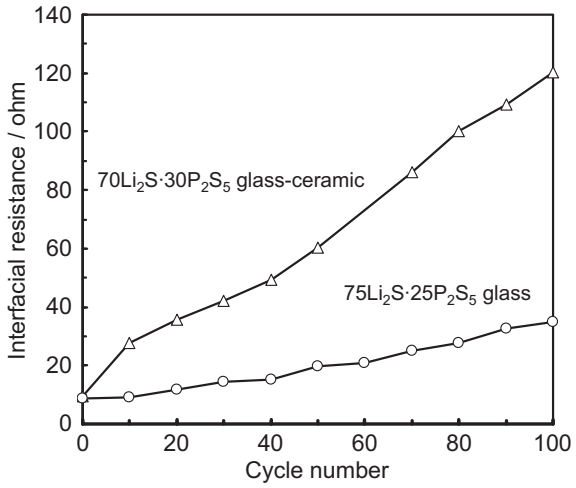

Fig. 5. Changes of interfacial resistance of the all-solid-state C/$LiCoO_2$ cells using the $70Li_2S{\cdot}30P_2S_5$ glass–ceramic and the $75Li_2S{\cdot}25P_2S_5$ glass during charge–discharge cycles at 60 °C. Measurements of interfacial resistance were conducted at a voltage of 4.0 V at room temperature.

60 °C under current density of 0.1 C. Cell voltages were adjusted by constant voltage charging at 4.0 V for 20 h before storage. The interfacial resistance of both cells increases during cycles. The interfacial resistance of the cell using the $70Li_2S{\cdot}30P_2S_5$ glass–ceramic increases rapidly compared to the cell using the $75Li_2S{\cdot}25P_2S_5$ glass. The resistance of the former cell increases after 100 cycles by a factor of 13, although that of the latter cell increases by a factor of 4. It is therefore estimated that the capacity retention of the cell using the $75Li_2S{\cdot}25P_2S_5$ glass was larger than that of the cell using the $70Li_2S{\cdot}30P_2S_5$glass–ceramic. On the other hand, changes of interfacial resistance between $LiCoO_2$ and sulfide solid electrolytes of the cells without charge–discharge cycles were investigated. The cells were kept under an open circuit at 60 °C after constant voltage charging at 4.0 V for 20 h. The results are shown in Fig. 6. The interfacial resistance of both cells gradually increases with increasing storage time at 60 °C without charge–discharge cycles. In addition, the interfacial resistance of the cell using the $70Li_2S{\cdot}30P_2S_5$ glass–ceramic increases rapidly compared to the cell using the $75Li_2S{\cdot}25P_2S_5$ glass.

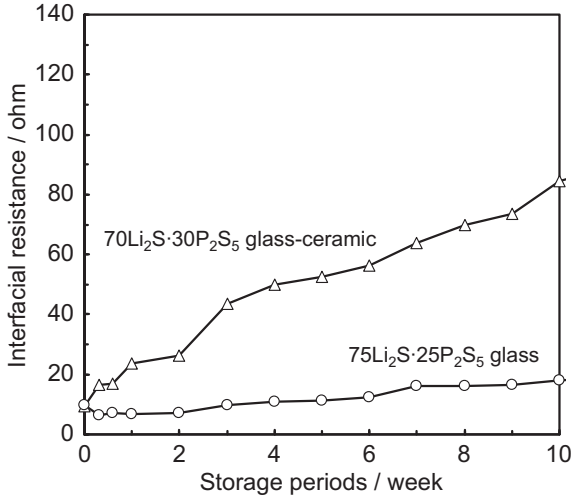

Fig. 6. Changes of interfacial resistances of the all-solid-state C/$LiCoO_2$ cells using the $70Li_2S{\cdot}30P_2S_5$ glass–ceramic and the $75Li_2S{\cdot}25P_2S_5$ glass during storage under an open circuit at 60 °C without charge–discharge cycles. Cell voltages were adjusted by constant voltage charging at 4.0 V for 20 h before storage.

Observation of the interface between $LiCoO_2$ and sulfide solid electrolytes was performed to investigate effects of different electrolytes on the interfacial resistance. Fig. 7(a) shows a cross-sectional high-angle annular dark field (HAADF) STEM image in the vicinity of the interface between $LiCoO_2$ and the $70Li_2S{\cdot}30P_2S_5$ glass–ceramic, which was kept under an open circuit at 60 °C for 4 weeks after constant voltage charging at 4.0 V for 20 h. Fig. 7(b) shows EDX line profiles for Co, Nb, P, and S elements at an arrow position shown in Fig. 7(a). Three layers of $LiCoO_2$, $LiNbO_3$, and the $70Li_2S{\cdot}30P_2S_5$ glass–ceramic are observed as shown in Fig. 7(a). Furthermore, an interfacial layer with a different contrast is visible between $LiCoO_2$ and $LiNbO_3$. Existence of small amounts of S and P elements is observed at the $LiCoO_2$ layer over a distance of 25 nm from the $LiCoO_2$/$LiNbO_3$ interface. Structural changes at the interface are expected to cause degradation of capacity with increasing interfacial resistance between $LiCoO_2$ and the $70Li_2S{\cdot}30P_2S_5$ glass–ceramic.

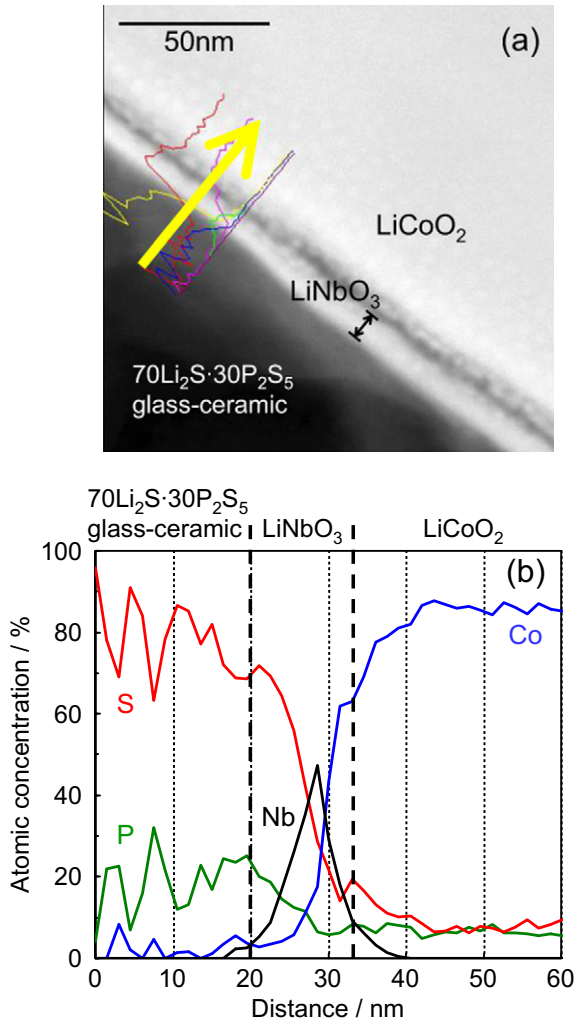

Fig. 7. (a) Cross-sectional HAADF-STEM image of the interface between the $70Li_2S{\cdot}30P_2S_5$ glass–ceramic and $LiCoO_2$ coated with $LiNbO_3$, which was kept under an open circuit at 60 °C for 4 weeks after constant voltage charging at 4.0 V for 20 h, and (b) cross-sectional EDX line profiles for Co, Nb, P, and S elements. The arrow in (a) indicates the position of EDX measurements.

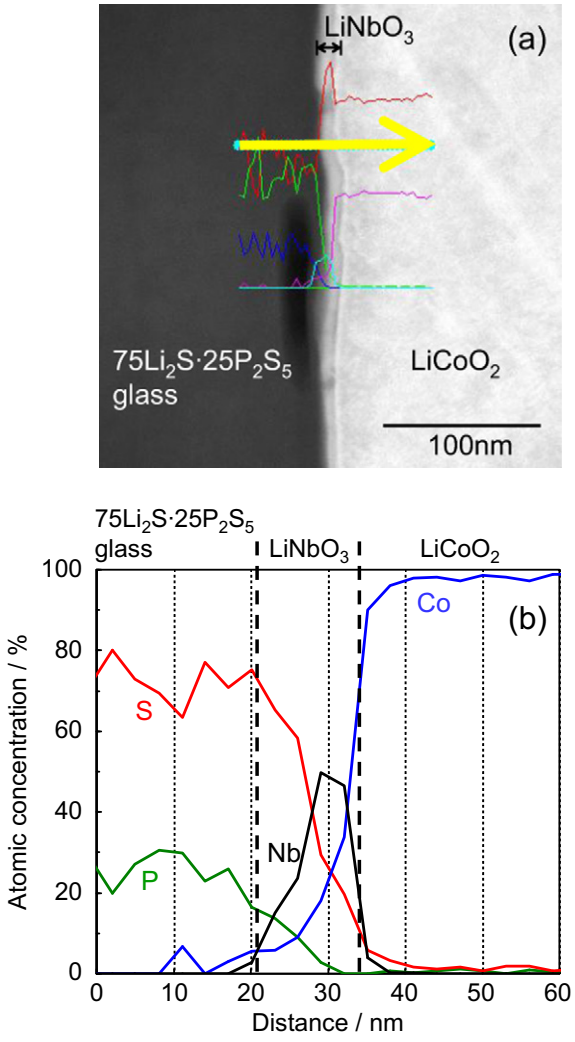

Fig. 8. (a) Cross-sectional HAADF-STEM image of the interface between the $75Li_2S{\cdot}25P_2S_5$ glass and $LiCoO_2$ coated with $LiNbO_3$, which was kept under an open circuit at 60 °C for 4 weeks after constant voltage charging at 4.0 V for 20 h, and (b) cross-sectional EDX line profiles for Co, Nb, P, and S elements. The arrow in (a) indicates the position of EDX measurements.

Fig. 8(a) shows a cross-sectional HAADF-STEM image near the interface between $LiCoO_2$ and the $75Li_2S{\cdot}25P_2S_5$ glass, which was kept under an open circuit at 60 °C for 4 weeks after constant voltage charging at 4.0 V for 20 h. Fig. 8(b) shows EDX line profiles for Co, Nb, P, and S elements at an arrow position in Fig. 8(a). Only three layers of interface of $LiCoO_2$, $LiNbO_3$, and the $75Li_2S{\cdot}25P_2S_5$ glass are detected as shown in Fig. 8(a). Moreover, existence of the S and P elements in the $LiCoO_2$ layer is not observed. The interface is not greatly deteriorated after storage at a high voltage of 4.0 V at 60 °C for 4 weeks, suggesting that less structural change could be brought about by high chemical stability of the $75Li_2S{\cdot}25P_2S_5$ glass. Therefore, the cell using the $75Li_2S{\cdot}25P_2S_5$ glass exhibited better cycle and storage performance.

4. Conclusions

Characteristics of sulfide solid electrolytes such as ion conductivity and chemical stability affected electrochemical performance of all-solid-state cells. Solid electrolytes with high conductivity were expected to contribute to the improvement of the rate performance of the cell because the $C/LiCoO_2$ cell using the $70Li_2S{\cdot}30P_2S_5$ glass–ceramic with high ion conductivity of 1.5×10^{-3} S cm^{-1} at room temperature showed good rate performance. On the other hand, solid electrolytes with high chemical stability enhanced the cell life because the $C/LiCoO_2$ cell using the $75Li_2S{\cdot}25P_2S_5$ glass with high chemical stability exhibited better cycle and storage performance. Therefore, the use of solid electrolytes with both high conductivity and high chemical stability was desired for improving battery performance.

References

[1] S. Kondo, K. Takada, Y. Yamamura, Solid State Ionics 53–56 (1992) 1183.
[2] M. Tatsumisago, K. Hirai, T. Minami, K. Takada, S. Kondo, J. Ceram. Soc. Jpn. 101 (1993) 1315.
[3] A. Hayashi, S. Hama, H. Morimoto, M. Tatsumisago, T. Minami, Chem. Lett. (2001) 872.
[4] F. Mizuno, A. Hayashi, K. Tadanaga, M. Tatsumisago, Solid State Ionics 177 (2006) 2721.
[5] R. Kanno, M. Murayama, J. Electrochem. Soc. 148 (2001) A742.
[6] N. Kamaya, K. Homma, Y. Yamakawa, M. Hirayama, R. Kanno, M. Yonemura, T. Kamiyama, Y. Kato, S. Hama, K. Kawamoto, A. Mitsui, Nat. Mater. 10 (2011) 682.
[7] H. Muramatsu, A. Hayashi, T. Ohtomo, S. Hama, M. Tatsumisago, Solid State Ionics 182 (2011) 116.
[8] F. Mizuno, A. Hayashi, K. Tadanaga, T. Minami, M. Tatsumisago, Chem. Lett. (2002) 1244.
[9] K. Minami, A. Hayashi, S. Ujiie, M. Tatsumisago, Solid State Ionics 192 (2011) 122.
[10] N. Ohta, K. Takada, I. Sakaguchi, L. Zhang, R. Ma, K. Fukuda, M. Osada, T. Sasaki, Electrochem. Commun. 9 (2007) 1486–1490.
[11] A. Sakuda, A. Hayashi, M. Tatsumisago, Chem. Mater. 22 (2010) 949.
[12] T. Minami, A. Hayashi, M. Tatsumisago, Solid State Ionics 177 (2006) 2715.